

Spatio-temporal dynamics and connectivity metrics of mangrove landscapes to prioritize coastal management in Sinjai Regency, Indonesia

Irwansyah^{1,2*}, Amran Saru³, Ambo Tuwo³, Muh. Hatta³, Nadiarti Nurdin Kadir^{4,5}, Ahmad Faizal³, Khairul Amri³

¹ Doctoral Program, Fisheries Science, Faculty of Marine Science and Fisheries, Universitas Hasanuddin, Jl. Perintis Kemerdekaan KM.10, Makassar 90245, South Sulawesi, Indonesia

² Faculty of Fisheries, Cokroaminoto Makassar University, Jl. Perintis Kemerdekaan KM.11, Makassar, 90245, South Sulawesi, Indonesia.

³ Department of Marine Science, Faculty of Marine Science and Fisheries, Universitas Hasanuddin, Jl. Perintis Kemerdekaan KM.10, Makassar 90245, South Sulawesi, Indonesia

⁴ Department of Fisheries, Faculty of Marine Science and Fisheries, Universitas Hasanuddin, Jl. Perintis Kemerdekaan KM.10, Makassar 90245, South Sulawesi, Indonesia

⁵ Aquatic Macrofaunal Biodiversity and Conservation (AMBioC) Research Group, Hasanuddin University, Jl. Perintis Kemerdekaan KM. 10, Makassar 90245, South Sulawesi, Indonesia

* Corresponding author's e-mail: wawansyah86@gmail.com

ABSTRACT

Mangrove ecosystems in Sinjai Regency, South Sulawesi, Indonesia, are increasingly exposed to coastal land-use conversion, aquaculture expansion, and biophysical pressures, yet explicit spatial evidence to guide restoration priorities remains limited. This study assessed the spatial and temporal dynamics of mangroves using Landsat SR imagery from 2005 to 2025. Six land-cover classes were mapped (mangrove, non-mangrove vegetation, rice fields, aquaculture ponds, built-up areas, and water bodies) through supervised classification, comparing the performance of three machine learning algorithms: Random Forest (RF), support vector machine (SVM), and extreme gradient boosting (XGBoost). Reliable classification accuracy was achieved with Kappa values exceeding 0.80. Mangrove extent declined from 267 ha in 2005 to 231 ha in 2025, representing a net loss of 36.09 ha. Over the same period, aquaculture ponds expanded by 74.79 ha and built-up areas increased by 13.59 ha, while water bodies decreased by 49.05 ha. Linear trend analysis indicated a consistent decline in mangrove extent, with an estimated loss rate of approximately 1.80 ha yr⁻¹ and a strong temporal fit ($R^2 = 0.72$). Landscape metrics revealed a decreasing number of mangrove patches and edge density, suggesting reduced ecosystem connectivity. Hotspot analysis provided a spatial basis for identifying management zones with high carbon stock potential and areas requiring restoration priority. By integrating remote sensing, land-cover transition analysis, and landscape metrics, this study offers a reproducible framework to support sustainable mangrove ecosystem management.

Keywords: land use land cover mangrove, google earth engine, machine learning, landscape metrics, mangrove degradation risk, management prioritization.

INTRODUCTION

Mangrove ecosystems provide critical ecological and socio-economic functions in tropical coastal landscapes such as carbon storage, shoreline protection from waves and storms, biodiversity support, and sustain fisheries,

provide access to coastal resources, and contribute to local well-being. These ecosystems are capable of storing large amounts of carbon, underscoring their importance for climate change mitigation (Kauffman et al., 2020; Goldberg et al., 2020; Fahmi et al., 2025; Fachrun et al., 2025;). The root structures and canopy of

mangroves significantly attenuate wave energy and tidal currents, thereby reducing coastal erosion and buffering shorelines from storm impact thereby lowering coastal erosion rates and mitigating storm damage (Krauss and Osland, 2020; Gijssman et al., 2021). Effective management of mangrove ecosystems has direct implications for livelihoods, community access to coastal resources, and the enhancement of local well-being (Damastuti and Groot, 2019).

Mangrove ecosystems are increasingly threatened by interacting anthropogenic and biophysical pressures that drive habitat loss, degradation, and fragmentation. Anthropogenic pressures such as coastal land conversion, aquaculture expansion, pollution, and illegal logging directly alter mangrove extent and spatial configuration, often producing smaller, more isolated patches (Newton, 2020; Williams, 2022). At the same time, biophysical stressors, including hydrological alteration, climate variability, and microclimatic shifts, can affect vegetation productivity, recruitment and regeneration capacity (Tinh et al., 2020; Chen et al., 2021; Vimal et al., 2021;). These pressures rarely operate independently; for example, eutrophication (Irwani et al., 2024) and coastal development may weaken mangrove structural resilience and accelerate the loss of ecosystem functions (Turschwell et al., 2020; Hagger et al., 2022). Consequently, conservation and restoration planning requires an integrated socio-ecological perspective that considers not only the extent of mangrove loss, but also changes in habitat fragmentation and connectivity

Habitat fragmentation is not merely a consequence of mangrove area loss, but also reflects changes in the spatial configuration of remaining forest patches. As continuous mangrove stands are converted into smaller and more isolated patches, ecological connectivity may decline, potentially affecting species movement, propagule dispersal, regeneration processes, carbon storage, and the long-term resilience of coastal ecosystems (Bryan-Brown et al., 2020; Asplund et al., 2021; Hagger et al., 2022;). Therefore, mangrove degradation assessments should move beyond total area change and incorporate landscape metrics that describe patch size, edge complexity, isolation, aggregation, and connectivity. Multi-temporal satellite imagery combined with spatial metrics can help identify where mangrove loss, fragmentation,

and partial recovery occur through time, providing spatial evidence for restoration prioritization, coastal conversion control, aquaculture regulation, and hydrological rehabilitation (Turschwell, 2020; Zhang et al., 2024)

In Sinjai Regency, South Sulawesi, mangroves form part of a dynamic coastal landscape where ecological functions and human land-use pressures intersect. These mangrove systems contribute to shoreline protection, fisheries habitat, carbon storage, and livelihood support for coastal communities, but they are increasingly exposed to aquaculture expansion, coastal development, terrestrial runoff, and hydrological modification. Such pressures may not only reduce mangrove extent, but also alter the spatial arrangement of remaining patches, with implications for landscape connectivity and restoration potential. Sinjai therefore provides a relevant local case for examining how long-term mangrove change, fragmentation, and connectivity can be translated into spatial priorities for coastal restoration and planning.

Although mangrove changes have been widely assessed using remote sensing, many studies remain focused primarily on estimating gains and losses in mangrove area. Less attention has been given to how changes in mangrove extent are accompanied by shifts in landscape configuration, fragmentation, and connectivity, particularly at local coastal-management scales. In Indonesia, and especially in smaller regency-level coastal landscapes such as Sinjai, spatially explicit evidence linking long-term mangrove dynamics, land-cover transitions, fragmentation metrics, and restoration priority areas remains limited. This knowledge gap constrains the ability of local managers to distinguish areas of persistent mangrove conversion from areas where remaining patches still retain functional connectivity or show potential for recovery.

Therefore, this study aims to assess spatio-temporal mangrove dynamics and landscape connectivity in Sinjai Regency from 2005 to 2025 using multi-temporal Landsat imagery, Google Earth Engine, Random Forest classification, transition analysis, and landscape metrics. Specifically, this study seeks to: (1) quantify changes in mangrove and other coastal land-cover classes; (2) identify land-cover transitions associated with mangrove loss and recovery; (3) evaluate fragmentation and connectivity patterns using

landscape metrics; and (4) identify priority areas for coastal restoration and spatial planning

METHODOLOGY

Study area

The study area is presented in Figure 1 and comprises both terrestrial and marine environments. The terrestrial boundary was defined based on the administrative boundaries of villages

Table 1. Training samples used for supervised classification

Training sample class	Number of sample units	Sampe area (ha)
Mangrove	29	54.88
Built-up area	28	33.69
Non-mangrove vegetation	38	176.02
Rice field	42	119.33
Water body	34	213.89
Aquaculture pond	18	172.11
Total	189	769.92

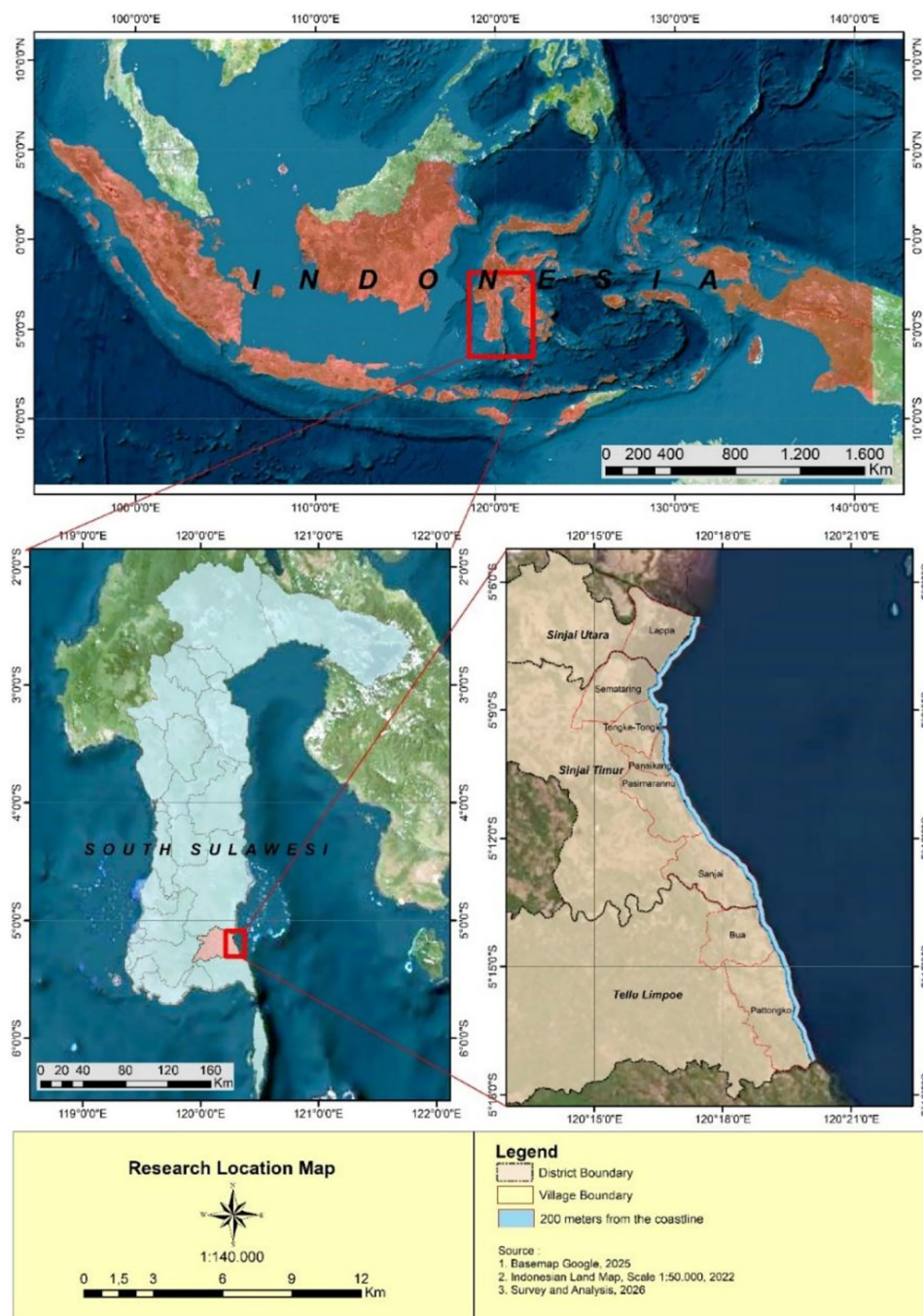


Figure 1. Map of research location

located within three coastal sub-districts of Sinjai Regency, namely North Sinjai, East Sinjai, and Tellulimpoe. North Sinjai Sub-district includes one village, namely Lappa Village. East Sinjai Sub-district consists of five villages: Sematar-ing, Tongke-Tongke, Panaikang, Pasimarannu, and Sanjai. Tellulimpoe Sub-district comprises two villages, namely Bua and Pattongko. The total terrestrial area covers 4,886 ha. The marine area was delineated by applying a 200 m buffer from the coastline, assuming this zone represents a potential mangrove ecosystem area and coastal protection zone. The marine area covers 732 ha, resulting in a total study area of 5,618 ha. These boundaries were subsequently used as the Area of Interest (AOI) for satellite image processing and spatial analysis.

Data sources

Primary satellite imagery data were collected using the Google Earth Engine platform (<https://earthengine.google.com>). The primary dataset consisted of Landsat Collection 2 Level 2 Surface Reflectance (SR) imagery, including Landsat 7 ETM+ and Landsat 8 OLI, with a spatial resolution of 30 m. Image acquisition was conducted for five observation years: 2005, 2010, 2015, 2020, and 2025. The training dataset was compiled from visual interpretation of Google Earth imagery (Supplementary material 1). As presented in Table 1, six land-cover classes were defined: mangrove, built-up area, non-mangrove vegetation, rice field, aquaculture pond, and water body. A total of 189 training samples covering 769.92 ha were used for the classification process.

Secondary data included shapefiles of the administrative boundaries of Sinjai Regency, sub-districts, villages, and the coastline. These datasets were obtained from the South Sulawesi

Provincial Spatial Planning Document provided by the local government.

Data processing and analysis

Land use/land cover classification

Land-use/land-cover (LULC) classification was conducted independently for each study year (2005, 2010, 2015, 2020, and 2025). The satellite imagery used was Landsat Surface Reflectance (SR) with relevant spectral bands (SR_B1, SR_B2, SR_B3, SR_B4, SR_B5, SR_B7). Pre-processing involved selecting annual image collections (January 1 – December 30), applying cloud and cloud-shadow masking to generate cloud-free composites, and compiling median values to reduce temporal noise and produce more representative imagery. Images were then clipped to the area of interest (AOI). Training samples were merged, and pixel values from relevant spectral bands were extracted to train the models prior to application. LULC classification was performed using supervised classification. Three machine learning algorithms were compared: Random Forest (RF) and support vector machine (SVM) implemented on the Google Earth Engine platform (Supplementary material 2), and extreme gradient boosting (XGBoost) implemented using the xgboost library in R Studio (Supplementary material 3). The RF classifier was executed with explicit parameters: number of trees = 500, mtry = default (number of variables per split), minLeafPopulation = 1, and bagFraction = 0.5. The SVM employed a radial basis function (RBF) kernel with cost = 10 and gamma = 0.5. XGBoost was run with max_depth = 6, eta = 0.1, subsample = 0.8, colsample_bytree = 0.8, and nrounds = 200. Model validation was performed using the 70/30 test split. Accuracy assessment included Overall accuracy (OA) and the Kappa coefficient, with Kappa >0.80

Table 2. Accuracy level of supervised classification using machine learning algorithms

Algorithm	Parameter	Year					Mean
		2005	2010	2015	2020	2025	
Random forest	Overall accuracy	0.84	0.88	0.88	0.91	0.92	0.886
	Kappa	0.8	0.86	0.84	0.88	0.9	0.856
SVM	Overall accuracy	0.25	0.25	0.28	0.27	0.26	0.262
	Kappa	0.18	0.17	0.16	0.23	0.26	0.20
XGBoost	Overall accuracy	0.84	0.88	0.88	0.91	0.92	0.886
	Kappa	0.8	0.85	0.83	0.87	0.9	0.85

considered the threshold for representative classification. In addition to internal validation, independent validation was conducted using 200 reference points derived from high-resolution Sentinel-2 imagery for the 2020 LULC classification (Supplementary material 4). Validation points were selected using stratified random sampling to ensure representation of all land cover classes. The classification outputs for each study year were exported in both raster (GeoTIFF) and vector (Shapefile) formats.

Statistical comparison of classification algorithms

Statistical analysis to examine differences in the performance levels of machine learning models Random Forest (RF), support vector machine (SVM), and extreme gradient boosting (XGBoost) was conducted using the RVAideMemoire library in RStudio (Supplementary Material 5). Data preparation involved adding a binary variable indicating correct predictions (1) and incorrect predictions (0), based on the actual class labels of each model's classification output. All results were merged into a single data frame, with sample identity (ID) serving as the observational block. For overall comparison across the three models, the data were reshaped into long format and analyzed using Cochran's Q Test. When the test results indicated statistical significance level, follow-up analyses were performed using pairwise McNemar tests to evaluate each algorithm pair (RF vs. SVM, RF vs. XGB, and SVM vs. XGB), thereby identifying which pairs differed significantly. The null hypothesis assumed no significant differences in classification accuracy among the competing algorithms. Statistical significance was consistently evaluated at the $\alpha = 0.05$ threshold

Scenario-based analysis of future mangrove dynamics

Future land-cover projections were generated using a Markov chain approach based on transition probabilities derived from land-cover maps (2005–2025). Two scenarios were evaluated: Business-as-usual (BAU) and conservation scenario (CS). Transition probabilities were calculated by harmonizing raster grids and analyzing the crosstab transition matrix for 2005–2025. The BAU scenario assumed that historical transition probabilities remained constant, whereas the CS scenario reduced the probability of mangrove conversion to other land

classes by 30% to represent conservation interventions. Projected mangrove extent for 2030 and 2035 was estimated by multiplying the scenario-specific transition probabilities with the baseline land-cover area in 2025 (Supplementary material 6).

Mangrove degradation risk mapping

Spatial degradation risk was assessed using landscape metrics derived from mangrove distribution maps. Risk levels were determined based on habitat degradation indicators, including the fragmentation index, edge density, and Euclidean Nearest Neighbor (ENN) distance. Each metric was standardized and integrated through a weighted overlay approach, with weights assigned using equal weighting. The resulting degradation risk index was classified into three categories: low, medium, and high risk. Areas characterized by high fragmentation, elevated edge density, and increased isolation were categorized as high-risk zones (Supplementary material 7). The resulting risk maps were used to identify priority areas requiring conservation interventions, connectivity enhancement, or ecological restoration programs.

Spatial statistical analysis

The classification results for each study year were further analyzed to evaluate LULC dynamics and landscape metrics. LULC dynamics were assessed by examining land cover transition patterns, net change, and the correlation between changes in mangrove cover and time. Landscape metrics were calculated to characterize mangrove landscape structure, including patch size, edge density, connectivity, and fragmentation index. Management zones for mangrove ecosystems were identified using a Random Forest machine learning model (ranger implementation) consisting of 500 trees, integrating LULC variables and landscape metrics as predictor variables. All spatial statistical analyses were conducted using libraries implemented in RStudio.

- Land cover transition and net change analysis – land cover transition analysis was conducted by extracting class statistics from the classified land-cover maps for 2005, 2010, 2015, 2020, and 2025. The number of pixels in each land cover class was calculated for each year and subsequently converted to area values based on the Landsat pixel resolution (30 × 30 m). Inter class transition analysis was

performed by aligning raster grids through resampling and generating raster stacks for consecutive periods (2005–2010, 2010–2015, 2015–2020, and 2020–2025). Transition matrices were constructed using cross tabulation to quantify land cover transitions between classes and calculate the area associated with each transition. Transition pivot tables were generated for each period to facilitate the interpretation of land-cover dynamics. Transition patterns were visualized using inter-class transition heatmaps. Net change for each land cover class during the 2005–2025 period was calculated and visualized to identify classes experiencing increases or decreases in area. For the mangrove class specifically, linear regression analysis was conducted to evaluate the relationship between mangrove extent and time (Supplementary material 8).

- Landscape metrics – raster data from land-cover classification were extracted based on the area of interest (AOI) and stored as a list. Landscape metrics were calculated exclusively for the mangrove class (0) by reclassifying mangrove pixels to a value of 1 and all other classes to 0, thereby producing a binary raster representing the spatial distribution of mangrove ecosystems. Landscape metrics were computed using the landscapemetrics package (version 2.2.1), with parameters including aggregation index, euclidean nearest neighbor (ENN) mean, mean patch size, number of patches, fragmentation index, and local edge density. Values for each metric parameter were summarized in tabular form and analyzed to identify trends in mangrove landscape metrics from 2005 to 2025 (Supplementary material 9).

Hotspot analysis for mangrove ecosystem management zones

Mangrove ecosystem management zones were determined using the Random Forest (ranger) machine learning algorithm. Predictors used to build hotspot models included land-cover classes and landscape metrics such as edge density, aggregation index, and fragmentation index. The combined input dataset was cleaned and oversampled to ensure balanced data distribution. Predictors were then applied to train the Random Forest model (ranger) with a robust set of 500 trees. Variable importance analysis was conducted prior

to predicting hotspot probabilities. Model outputs were categorized into two management zones: (i) hotspots with large patch sizes, recommended as zones of potential carbon stock, and (ii) hotspots with high edge density and fragmentation values, recommended as restoration zones to enhance local protection areas (Supplementary material 10). Final outputs were exported in raster (GeoTIFF) and vector (Shapefile) formats for further processing in ArcGIS.

RESULTS AND DISCUSSION

Results

Accuracy of machine learning algorithms for supervised land use/land cover classification

The accuracy assessment of LULC classification using the RF, SVM, and XGBoost machine learning algorithms is presented in Table 2. The RF and XGBoost models yielded nearly identical average values, with an Overall Accuracy of 0.89 and a Kappa coefficient of 0.86. Accuracy parameters demonstrated an increasing trend across the study years. In contrast, the SVM model produced substantially lower values, with an average Overall Accuracy of only 0.26 and a Kappa coefficient far below the representative threshold, at 0.02. Independent validation further confirmed the reliability of the classification results, yielding an Overall Accuracy of 0.87 and a Kappa coefficient of 0.74. For the mangrove class specifically, Producer's Accuracy reached 0.98 and User's Accuracy 0.86, indicating that the Random Forest model was able to identify mangrove areas with high reliability even when evaluated against external reference data.

The accuracy assessment of supervised land-cover classification using Google Earth Engine and the Random Forest machine learning algorithm for mangrove ecosystems in Sinjai Regency is presented in Table 3. The average values of Producer's Accuracy and User's Accuracy were calculated across six land-cover classes. The non-mangrove vegetation class achieved the highest Producer's Accuracy (0.94), while the built-up class recorded the lowest (0.69). The mangrove class showed relatively high accuracy with a value of 0.82.

Table 3. Class-based accuracy using the Random Forest algorithm

Year	Land cover class	Confusion matrix	Producer's accuracy (%)	User's accuracy (%)
2005	Mangrove (0)	131	0.70	0.90
	Built-up area (1)	58	0.51	0.65
	Non-mangrove vegetation (2)	533	0.93	0.90
	Ric field (3)	322	0.86	0.84
	Water body (4)	436	0.85	0.81
	Aquaculture pond (5)	485	0.84	0.80
2010	Mangrove (0)	145	0.75	0.89
	Built-up area (1)	67	0.56	0.84
	Non-mangrove vegetation (2)	554	0.93	0.90
	Ric field (3)	325	0.83	0.83
	Water body (4)	501	0.91	0.91
	Aquaculture pond (5)	557	0.94	0.87
2015	Mangrove (0)	159	0.86	0.93
	Built-up area (1)	75	0.61	0.74
	Non-mangrove vegetation (2)	532	0.95	0.95
	Ric field (3)	354	0.92	0.91
	Water body (4)	439	0.84	0.84
	Aquaculture pond (5)	482	0.86	0.82
2020	Mangrove (0)	168	0.89	0.97
	Built-up area (1)	96	0.90	0.96
	Non-mangrove vegetation (2)	577	0.95	0.94
	Ric field (3)	359	0.90	0.90
	Water body (4)	497	0.89	0.87
	Aquaculture pond (5)	510	0.89	0.91
2025	Mangrove (0)	180	0.92	0.96
	Built-up area (1)	92	0.91	0.92
	Non-mangrove vegetation (2)	553	0.96	0.95
	Ric field (3)	379	0.94	0.90
	Water body (4)	474	0.88	0.88
	Aquaculture pond (5)	511	0.87	0.89

Land cover in the mangrove ecosystem of Sinjai Regency

The area of each land cover class is presented in Table 4. while the spatial distribution patterns are shown in Figure 2. Among the identified land-cover classes. non-mangrove vegetation represented the dominant class. with an average area of 2.314.80 ha. accounting for approximately 41.20% of the total study area. Non-mangrove vegetation exhibited a declining trend over the study period. decreasing from 2.415 ha in 2005 to 2.267 ha in 2025. This land cover class was predominantly distributed in the southern part of the study area. particularly within East Sinjai and Tellulimpoe Sub-districts. Mangrove cover represented the smallest land

cover class. with an average area of 240.80 ha. corresponding to approximately 4.28% of the total study area. Mangrove ecosystems were primarily distributed in the northern coastal zone. particularly within North Sinjai and East Sinjai Sub-districts. including Semataring. Tongke-Tongke. and Panaikang Villages.

Built-up areas were most extensively distributed in North Sinjai Sub-district. which serves as the administrative center of the regency. with an average area of 260.20 ha. representing approximately 4.60% of the study area. Aquaculture ponds were concentrated in North Sinjai and East Sinjai Sub-districts. covering approximately 689.80 ha or 12.27% of the total study area. Rice fields were distributed relatively

Table 4. Area of land cover classes

Land cover class	2005	2010	2015	2020	2025	Mean
Mangrove	267	239	240	227	231	240.80
Built-up area	227	246	313	275	240	260.20
Non mangrove vegetation	2415	2289	2386	2217	2267	2314.80
Rice field	1351	1428	1326	1498	1496	1419.80
Water body	692	690	724	711	643	692.00
Aquaculture pond	666	725	628	689	741	689.80

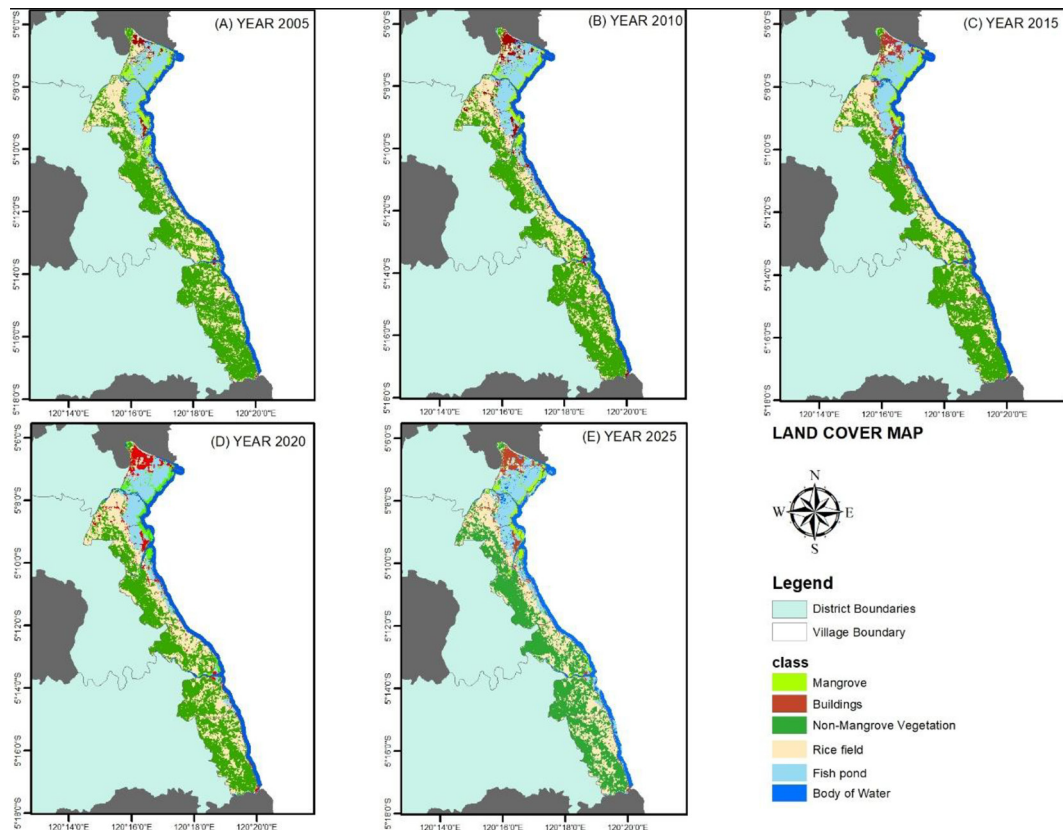


Figure 2. Land cover based on year

evenly across all sub-districts. with an average area of 692.00 ha. accounting for approximately 25.27% of the study area.

Land cover transition and net change

The results of the land cover transition analysis for the period 2005–2025 are presented in Figure 3a. The average proportion of land cover transition among all classes was 23.42%. The highest transition rate was observed in the water body class, with 37.80% of its area changing during the study period, whereas the non-mangrove vegetation class exhibited the lowest transition rate at 12.57%. Mangrove ecosystems experienced a

relatively high level of land-cover transition, with 32.15% of the mangrove area changing to other land cover classes. Similar transition rates were observed for built-up areas (32.15%), while rice fields and aquaculture ponds exhibited transition rates of 19.23% and 13.12%, respectively.

The largest gains in mangrove area were associated with transitions from non-mangrove vegetation, contributing approximately 15.6 ha, followed by aquaculture ponds (13.8 ha) and water bodies (13.7 ha). Conversion from built-up areas to mangroves was minimal, accounting for only 0.3 ha, whereas conversion from rice fields to mangroves contributed approximately 6.8 ha. Conversely, the largest losses of mangrove area

resulted from transitions to non-mangrove vegetation, totaling 19.2 ha. The smallest transition was observed from mangroves to built-up areas, accounting for only 0.6 ha. Mangrove conversion to aquaculture ponds represented a substantial transition, covering 17.6 ha, while conversion to rice fields accounted for 8.2 ha. In addition, mangrove conversion to water bodies totaled 6.1 ha.

Net changes in land-cover classes between 2005 and 2025 are presented in Figure 3b. The largest increase was observed in the rice field class, which expanded by 144.81 ha during the study period, followed by aquaculture ponds with an increase of 74.79 ha. Built-up areas also exhibited a positive net change, increasing by 13.59 ha. In contrast, water bodies, mangroves, and non-mangrove vegetation experienced net losses in area. Non-mangrove vegetation showed the largest decline, decreasing by 148.05 ha, followed by water bodies, which decreased by 49.05 ha. Mangrove cover also declined considerably, with a net loss of 36.09 ha, equivalent to approximately 1.80 ha year⁻¹. The linear regression analysis presented

in Figure 4 yielded the regression equation $y = 3.63 \times 10^3 - 1.68x$ with an R^2 value of 0.72, indicating a substantial declining trend in mangrove extent over the study period.

Landscape metrics

Landscape metric analysis is presented in Figure 5. The number of mangrove patches showed a declining trend from 2005 to 2025, decreasing from 402 to 317. Patch dynamics were observed, with an increase between 2005 and 2010, followed by a significant decline until 2020, reaching 291 patches. A slight recovery occurred in 2025, with the number rising to 317. The reduction in patch numbers, particularly small patches vulnerable to fragmentation, left larger patches dominating the landscape. The mean patch size exhibited an overall increasing trend, rising from 13.97 ha in 2005 to 19.30 ha in 2020, before declining to 17.71 ha in 2025. This increase in patch size reflects greater landscape aggregation, which rose from 79.97 in 2005 to 84.38 in 2020, followed

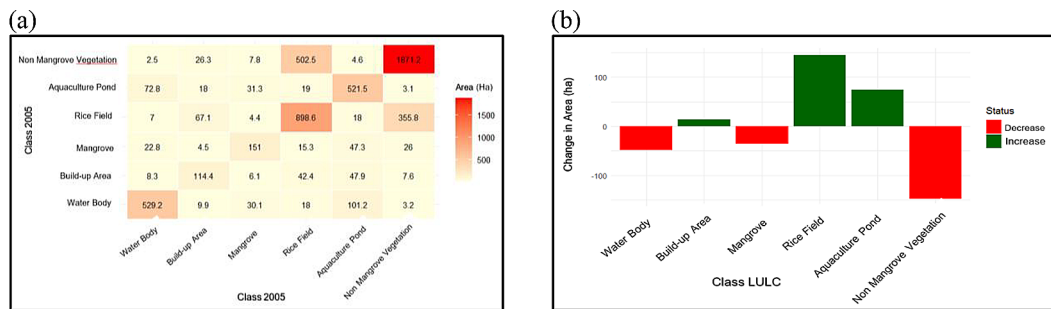


Figure 3. Dynamics of land cover changes: (a) land cover transition matrix for the 2005-2025 period; (b) net change in land cover from 2005 to 2025

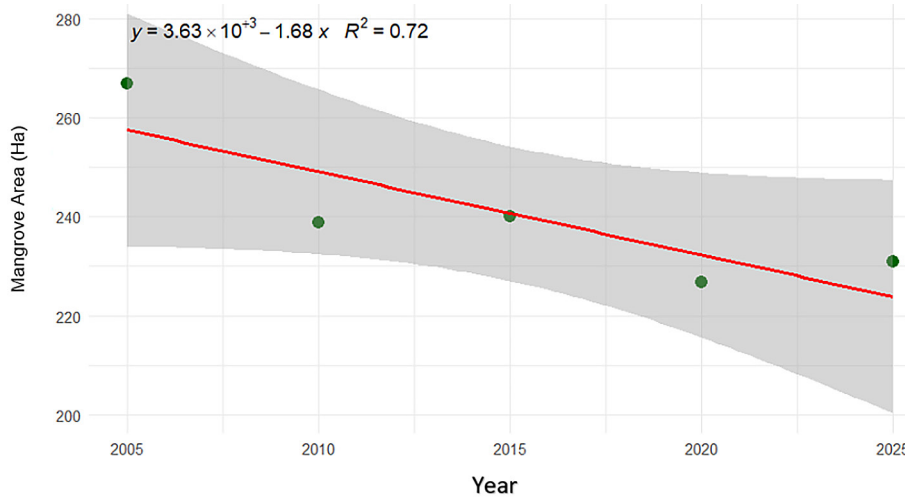


Figure 4. Linear regression of changes in mangrove cover over time

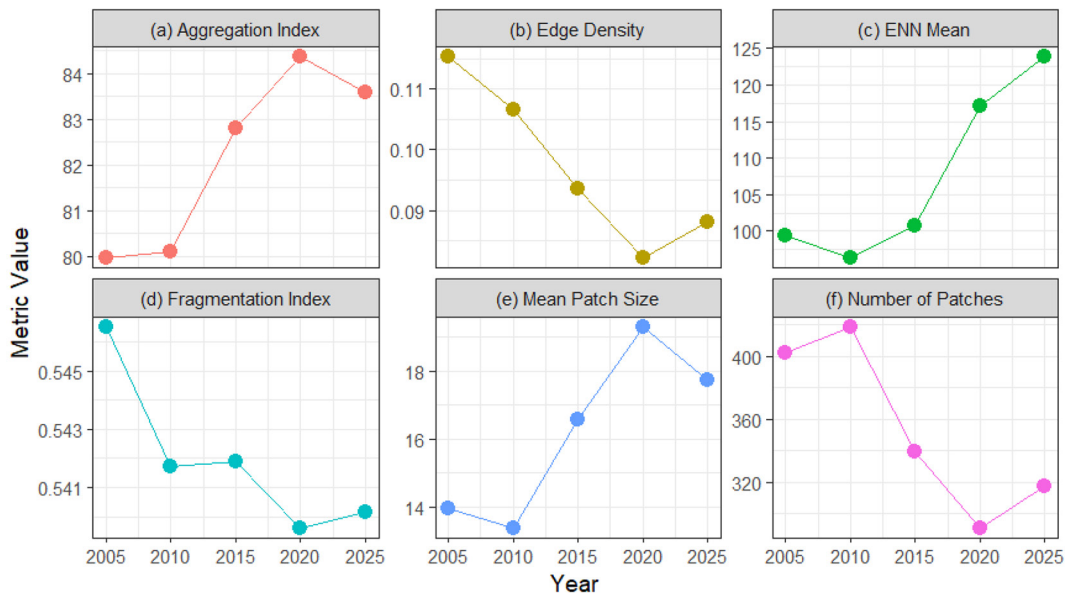


Figure 5. Landscape metric penutupan lahan mangrove (a); aggregation index; (b) edge density; (c) ENN mean; (d) fragmentation index; (e) mean patch size dan (f) number of patch

by a slight decrease to 83.58 in 2025. The loss of small patches, which often serve as connectors between larger patches, contributed to an increase in Euclidean Nearest Neighbor (ENN) distance, from 99.42 m in 2005 to 123.90 m in 2025. Edge density showed a declining trend, dropping from 0.115 in 2005 to 0.082 in 2020, with a slight increase to 0.088 in 2025. The fragmentation index remained relatively stable, showing only a minor decrease from 0.546 in 2005 to 0.540 in 2025.

Mangrove ecosystem management zones

The analysis of the Random Forest machine learning algorithm in determining mangrove management hotspot zones, based on predictors of land-cover change and landscape metrics, revealed that the aggregation index had the highest importance value (17.038), followed by edge

density (10.655) and the fragmentation index (10.257). Land-use change predictors showed relatively lower importance values, with 3.367 for 2005 and 4.718 for 2020. The variable importance values of the Random Forest model are presented in Table 5.

The extent and distribution of mangrove management zones are shown in Figure 6. Hotspot analysis categorized the recommendations into two management zones: (i) zones with high aggregation and large patch sizes, suitable for management aimed at potential carbon stock, and (ii) zones with high edge density and fragmentation, recommended for restoration to strengthen local protection areas. The potential carbon stock zone within the mangrove ecosystem of Sinjai Regency covers 133.13 ha, primarily distributed in the northern region, specifically in Sinjai Utara and Sinjai Timur Districts. In contrast, the restoration zone covers approximately 66.99 ha, concentrated in the northern area but forming smaller patches extending southward.

Table 5. Variable importance values of the Random Forest hotspot model for mangrove ecosystem management zones

Variable	Importance
LULC 2005	3.367
LULC 2010	0.599
LULC 2015	1.884
LULC 2020	4.718
Edge density	10.655
Aggregation	17.038
Fragmentasi	10.257

Discussion

Accuracy of machine learning-based classification

The dynamics of land-cover and land-use change in relation to natural resources occur rapidly, thereby increasing the demand for accurate LULC estimation. The availability of large

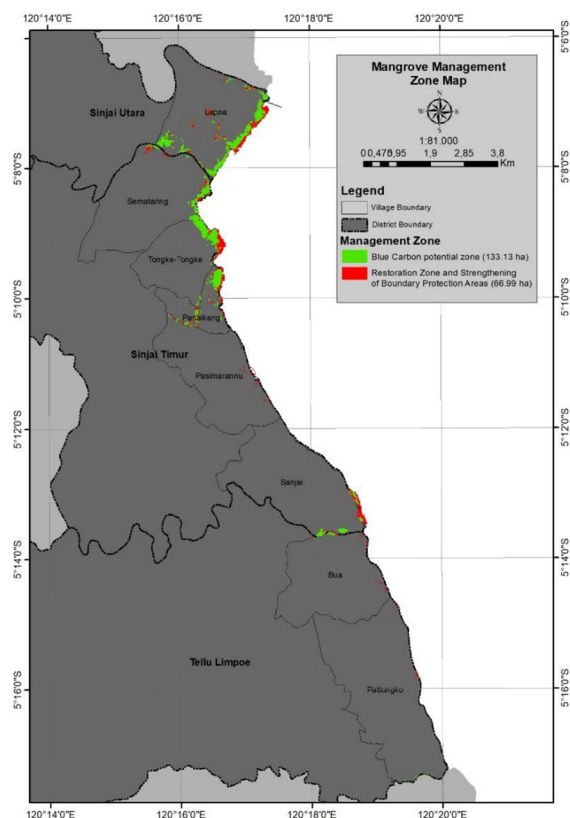


Figure 6. Spatial distribution of mangrove ecosystem management zones, highlighting areas designated for blue carbon development and restoration to strengthen local protection

datasets over extended time periods requires machine learning approaches to process data more efficiently and accurately (Ahmed, 2023). The integration of machine learning algorithms within google earth engine (GEE) has been demonstrated to enhance the accuracy of LULC classification methods (Bayrakdar et al., 2022; Kafle et al., 2023; Pande et al., 2024). Accuracy values are critical as the basis for interpreting classification results, since they directly influence decision-making in land resource management planning.

The average overall accuracy and Kappa values of the Random Forest and XGBoost algorithms were highly similar, with Overall Accuracy ≈ 0.89 and Kappa ≈ 0.86 , indicating a high level of reliability. In contrast, the SVM algorithm produced values below the acceptable threshold. Comparable findings were reported by Bogale et al., (2025), where RF achieved the highest accuracy, while SVM recorded the lowest compared to other algorithms such as CART and GTB. It has been further emphasized that the choice of machine learning algorithm strongly depends on the characteristics of the dataset (Patil and Panhalkar,

2023; Pande et al., 2024). Beyond algorithm selection, differences in LULC classification accuracy are also influenced by factors such as image resolution (Basheer, 2022; Ahmed, 2023) and the number and distribution of samples. Imbalanced class distribution can reduce both Producer's Accuracy and User's Accuracy (Zhao, 2020). In addition to accuracy values, it is equally important to interpret classification results through spatial validation, examining spatial patterns generated by statistical analysis (Feizizadeh, 2023).

Statistical comparison of classification algorithms

The statistical comparison of the three classification algorithms (Random Forest, support vector machine, and extreme gradient boosting) using Cochran's Q Test yielded a test statistic of $Q = 2971.24$ with degrees of freedom ($df = 2$) and a p -value $< 2.2e-16$, indicating a statistically significant difference among the algorithms ($p < 0.05$). The estimated probability of correct classification was 0.918 for RF and 0.919 for XGBoost, demonstrating nearly identical accuracy levels, both substantially higher than the SVM model, which achieved a probability of 0.262. Results of the pairwise McNemar's test (Figure 7) showed that the difference between RF and XGBoost was not statistically significant ($p = 0.922$), whereas both models differed significantly from SVM ($p < 0.001$). These findings indicate that although Random Forest achieved the highest Overall Accuracy and Kappa coefficient, the practical difference between RF and XGBoost is relatively small. Therefore, algorithm selection should consider not only classification accuracy but also model complexity, computational efficiency, and implementation requirements.

LULC dynamics and landscape metrics

As resources of considerable value, mangrove ecosystems are highly vulnerable to natural processes such as erosion, sedimentation, and natural disasters. In addition, they face intense anthropogenic pressures driven by urban growth, resource exploitation, and pollution release. Population growth accompanied by increased economic activity has accelerated the transformation of land use/land cover (Hoque, 2022; El Yousfi et al., 2025). Urbanization rate and infrastructure demands are major drivers of LULC change, reflecting regional development processes (Djafar et al.,

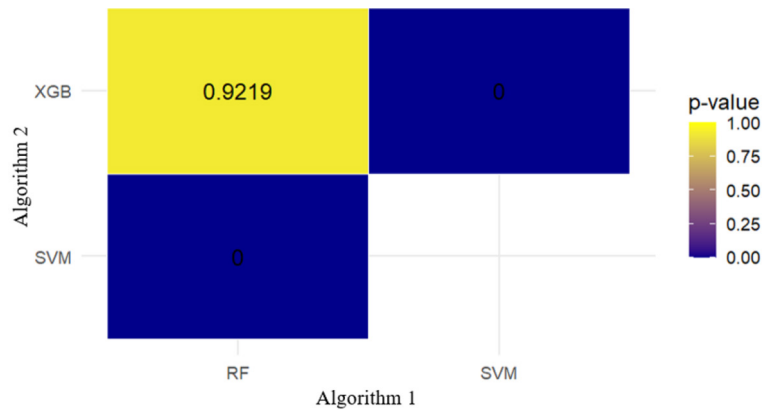


Figure 7. Pairwise statistical testing of Random Forest (RF), Support vector machine (SVM), and Extreme gradient boosting (XGB) classification models

2026). Human activities thus exert both direct and indirect impacts on these ecosystems. At the global scale, mangrove ecosystems have shown a declining trend of approximately 1–2% annually (Gilani, 2021), which has significant implications for ecosystem functions related to climate mitigation, particularly carbon stock provision (Sharma et al., 2020; Ernawati et al., 2024). Furthermore, the degradation of ecosystem structure reduces ecosystem services, indirectly affecting the well-being of local communities (Newton, 2020; Sardar, 2021). By altering ecological processes and ecosystem functions, LULC change fragments habitats, diminishes terrestrial carbon storage, increases soil erosion, and reduces opportunities for recreation and ecotourism (Li et al., 2022).

Understanding patterns of landscape dynamics is one of the most important approaches in landscape ecology, as it establishes the relationship between ecological processes and landscape configuration. Examining the dynamics of landscape fragmentation reveals the internal patterns of landscape change and succession, serving as a key indicator of how mangrove stands influence ecosystem habitats, species diversity, and carbon storage capacity (Sardar, 2021; Kanniah, 2021). Deforestation rates cannot always be directly associated with fragmentation levels, since the strength of the relationship varies regionally. Changes in fragmentation may lead to either increases or decreases in patch size when mangrove loss occurs (Bryan-Brown et al., 2020).

Land-use and land-cover change over time and across different locations is influenced by multiple factors, including social, economic, and natural ecological conditions (Liu et al., 2020). Ecosystem dynamics are inevitable, making it

essential to understand the concept of ecosystem change as a basis for decision-making in ecosystem management. LULC dynamics serve as an important indicator for identifying patterns of change within an ecosystem. Evaluating LULC dynamics can assist institutions in making strategic decisions related to mangrove conservation, helping to prevent degradation and deforestation through the development of sustainable management plans (El Yousfi et al., 2025; Gilani, 2021; Sardar, 2021).

Future mangrove dynamics under alternative scenarios

The projected extent of mangrove ecosystems shows a marked contrast between scenarios (Figure 8). Under the Business-as-Usual (BAU) scenario, mangrove area exhibits a declining trend, whereas under the Conservation Scenario (CS), mangrove extent shows a slight increase. In the BAU scenario, mangrove cover is projected to decrease from 230.8 ha in 2025 to 212.2 ha in 2030 (–8.05%), and further to 202.9 ha in 2035 (–27.9 ha), representing an average annual decline of 2.01% from 2025. This trend reflects the continuation of historical land-use transitions, particularly the conversion of mangroves into aquaculture ponds and other coastal uses.

In contrast, the CS scenario indicates a modest increase in mangrove extent, with projections of 231.7 ha in 2030 (+0.38%) and 233.0 ha in 2035 (+0.95%) relative to 2025. Compared to BAU, the CS scenario prevents approximately 19.5 ha of mangrove loss by 2030 and 30.1 ha by 2035. Spatially, the largest differences between scenarios occur in coastal and riverine zones, where fragmentation pressures are most intense.

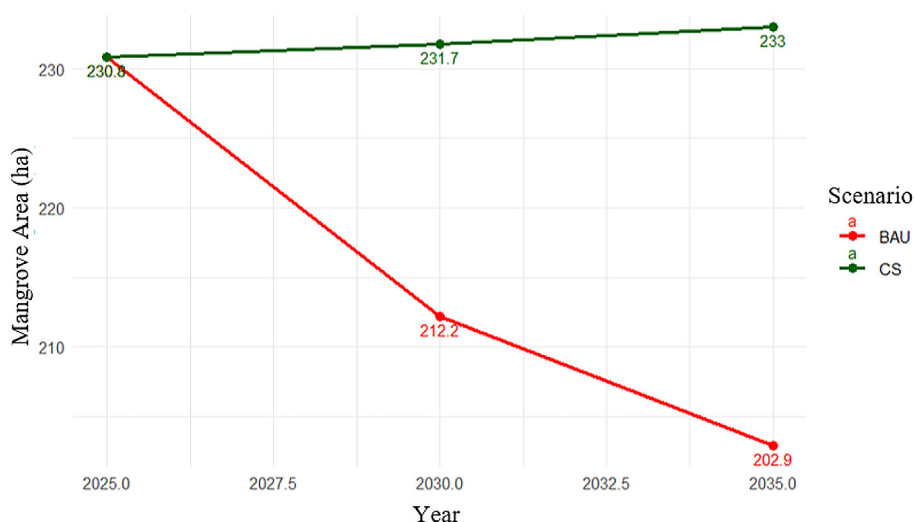


Figure 8. Projected mangrove extent under BAU and CS scenarios

These findings highlight that targeted conservation interventions can substantially enhance the long-term sustainability of mangrove ecosystems in the study area.

Zoning approaches for mangrove ecosystem management

Mangrove forest management faces complex challenges involving social, ecological, and economic dimensions that require targeted strategies and measurable management programs to achieve long term sustainability objectives (Arifanti et al., 2022). Sustainable development depends on understanding future demands for, and availability of, land based natural resources. In this context, modeling approaches have become valuable tools for predicting potential land use changes under different management scenarios (Hoque, 2020). Conservation efforts can be strengthened through spatial analyses that integrate multiple sources of information, including geospatial data, remote sensing products, and climate and marine modeling outputs (Maurya et al., 2021; Syahid et al., 2023).

A zoning-based approach is particularly important in mangrove ecosystem management because the supply and demand of ecosystem services often vary across space. Consequently, managing spatial heterogeneity requires the evaluation and zoning of ecosystem services to support effective decision-making (Sobhani and Danekar, 2023). The management zones identified in this study, based on LULC dynamics and landscape metrics, indicate that high-priority management areas are predominantly located along ecosystem boundaries,

particularly in coastal margins and riverine zones. This spatial pattern suggests that management priorities are closely associated with areas experiencing greater ecological pressures and landscape change. Management and conservation interventions are therefore essential to halt ecosystem decline, maintain ecosystem integrity, and preserve ecological and socio-economic functions. The identification of priority management zones provides a spatially explicit basis for directing restoration and conservation efforts toward areas that are potentially more vulnerable to degradation and fragmentation.

Mangrove degradation risk assessment

The risk assessment based on landscape metrics revealed non-linear dynamics over time. The mangrove risk index (Figure 9) was high in 2005, reflecting fragmented patch conditions and strong edge effects along the coastline. This elevated index indicates heightened vulnerability of the mangrove ecosystem. The index declined steadily until 2020, reaching a low level that suggests improved ecosystem stability. However, by 2025 the risk index increased again to a moderate level. The resulting risk map (Figure 10) shows that mangrove areas classified as high risk cover 17.91 ha, medium risk 96.03 ha, and low risk 50.40 ha. This spatially explicit risk assessment provides a basis for prioritizing restoration measures and enhancing connectivity in areas most affected by mangrove degradation.

Decision-making in mangrove conservation and management is inherently challenging because it involves multiple stakeholders, ranging

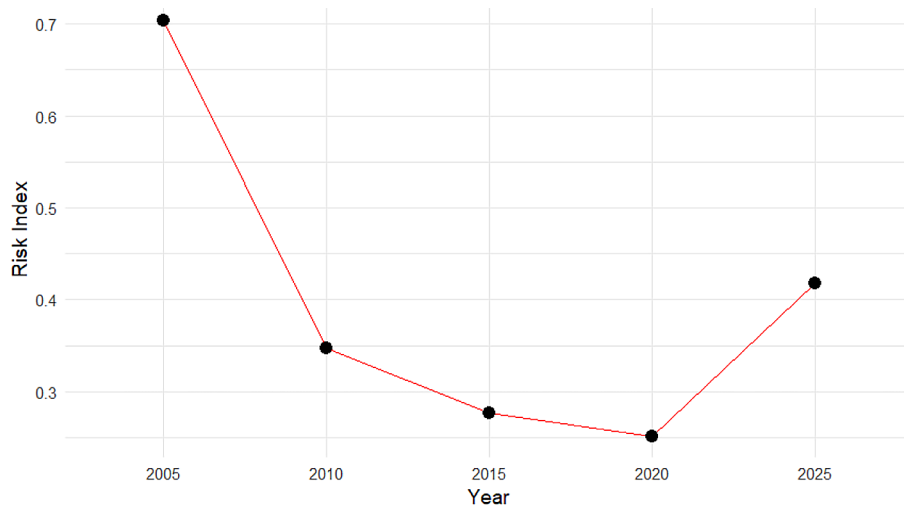


Figure 9. Average mangrove degradation risk index for 2005–2025

from government agencies to local communities (Trialfhianty et al., 2022). One of the most common challenges associated with zoning-based resource management is the occurrence of competing land use interests. Inadequate conflict resolution may reduce the effectiveness of management interventions and contribute to further resource degradation. Biodiversity conservation policies in mangrove ecosystems are unlikely to succeed without incorporating local livelihoods and community interests into planning and management frameworks (Ashton, 2022). Local communities play a critical role in ecosystem restoration, particularly through the application of traditional ecological knowledge that can support adaptive and context-specific management strategies (Ravaoarinosihoarana et al., 2023).

The statistical comparison demonstrated that Random Forest and XGBoost achieved similar classification performance, suggesting that both algorithms are suitable for LULC mapping in mangrove-dominated coastal environments. The limited difference between the models indicates that classification accuracy may be more strongly influenced by data quality, sample distribution, and feature selection than by algorithm choice alone. This finding is consistent with previous studies reporting comparable performance among ensemble machine-learning approaches when applied to medium-resolution satellite imagery.

The scenario analysis extends the study beyond retrospective landscape assessment by providing insight into potential future ecosystem trajectories. The projected decline in mangrove extent under the Business-as-Usual scenario suggests that ongoing land-use pressures may

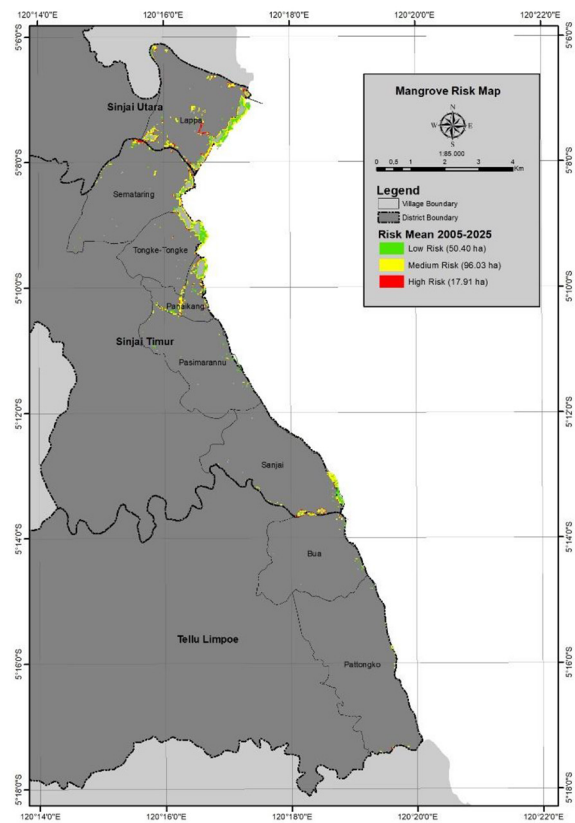


Figure 10. Mangrove degradation risk map

continue to reduce ecosystem integrity if no additional management measures are implemented. In contrast, the Conservation Scenario demonstrates that relatively modest reductions in mangrove conversion rates could substantially improve ecosystem persistence. These results highlight the importance of integrating land-use planning and restoration programs into long-term coastal management strategies.

The degradation-risk map complements the hotspot zoning analysis by identifying locations where ecological pressures are currently most intense. Areas characterized by high fragmentation, elevated edge density, and increased patch isolation are likely to experience reduced ecological resilience and greater vulnerability to future disturbances. Consequently, these areas should be prioritized for restoration, connectivity enhancement, and conservation interventions. The integration of risk assessment with landscape metrics provides a more comprehensive framework for management-oriented decision-making in mangrove ecosystems.

CONCLUSIONS

Based on the results of the study using LULC and landscape metrics, it can be concluded that the mangrove ecosystem in Sinjai Regency has experienced a significant decline in area over the past two decades. This reduction is primarily driven by local economic activities, including the expansion of aquaculture ponds and coastal development. The decline in mangrove area has direct impacts on the structure and function of the ecosystem. Reduced patch connectivity and increased fragmentation diminish the ecosystem's capacity to provide critical environmental services such as blue carbon storage, shoreline protection, and habitat for coastal biota. Given these ecosystem dynamics, the implementation of adaptive and sustainable mangrove management policies in Sinjai Regency is urgently required.

REFERENCES

- Ahmed, S. A. (2023). Land use and land cover classification using machine learning algorithms in google earth engine. *Earth Science Informatics*. <https://doi.org/10.1007/s12145-023-01073-w>
- Arifanti, V. B., Sidik, F., Mulyanto, B., Susilowati, A.,... (2022). Challenges and strategies for sustainable mangrove management in Indonesia: A review. In *Forests*. [mdpi.com](https://www.mdpi.com/1999-4907/13/5/695). <https://www.mdpi.com/1999-4907/13/5/695>
- Ashton, E. C. (2022). Threats to mangroves and conservation strategies. *Mangroves: Biodiversity, Livelihoods and Conservation*. https://doi.org/10.1007/978-981-19-0519-3_10
- Asplund, M. E., Dahl, M., Ismail, R. O., Arias-Ortiz, A.,... (2021). Dynamics and fate of blue carbon in a mangrove–seagrass seascape: influence of landscape configuration and land-use change. In *Landscape Ecology*. Springer. <https://doi.org/10.1007/s10980-021-01216-8>
- Basheer, S. (2022). Comparison of land use land cover classifiers using different satellite imagery and machine learning techniques. *Remote Sensing*, 14(19). <https://doi.org/10.3390/rs14194978>
- Bayrakdar, H. Y., Kavlak, M. Ö., Yılmazel, B.,... (2022). Assessing the performance of machine learning algorithms in Google Earth Engine for land use and land cover analysis: A case study of Muğla province, Türkiye. *Journal of Design for Resilience*. <http://www.drarch.org/index.php/drarch/article/view/98>
- Bogale, T., Degefa, S., Dalle, G., Abebe, G. (2025). Machine learning-based analysis of land use and land cover trends in southeastern Ethiopia using Google Earth Engine. In *Discover Sustainability*. Springer. <https://doi.org/10.1007/s43621-025-01709-5>
- Bryan-Brown, D. N., Connolly, R. M., Richards, D. R.,... (2020). Global trends in mangrove forest fragmentation. In *Scientific reports*. [nature.com](https://www.nature.com/articles/s41598-020-63880-1). <https://www.nature.com/articles/s41598-020-63880-1>
- Chen, L., Fan, H., Su, Z., Lin, Q.,... (2021). Enhancing carbon storage in mangrove ecosystems of China through sustainable restoration and aquaculture actions. *Wetland Carbon and Environmental Management*. <https://doi.org/10.1002/9781119639305.ch6>
- Damastuti, E., Groot, R. de. (2019). Participatory ecosystem service mapping to enhance community-based mangrove rehabilitation and management in Demak, Indonesia. In *Regional Environmental Change*. Springer. <https://doi.org/10.1007/s10113-018-1378-7>
- Djafar, N. W. R. E. M. I., Soma, A. S., Achmad, M., Hakiki, L. K. (2026). Land cover change and urban growth in north Gorontalo Regency using Sentinel-2 imagery. *Ecological Engineering & Environmental Technology*, 27(3), 341–367. <https://doi.org/10.12912/27197050/218187>
- El Yousfi, M., El Ghoulbzouri, A., Himi, M. (2025). Land-use land-cover change analysis using remote sensing and geographic information systems in northern Rif, Morocco. *Ecological Engineering & Environmental Technology*, 26(9), 121–137. <https://doi.org/10.12912/27197050/209558>
- Ernawati, N. M., Astarini, I. A., Suarna, I. W., Asyaktur, A. R., Perwira, I. Y., Dewi, A. P. W. K., Sugiana, I. P. (2024). Comparison of soil carbon-nitrogen ratio at two different mangrove ecosystem in Bali, Indonesia. *Ecological Engineering & Environmental Technology*, 25(7), 343–354. <https://doi.org/10.12912/27197050/188738>
- Fachrun, A., Rukmana, D., Idrus, R. (2025). Climate change control potential of mangrove ecosystems in Rawa Aopa Watumohai National Park, Tinanggea District. *Ecological Engineering &*

- Environmental Technology*, 26(1), 379–387. <https://doi.org/10.12912/27197050/196088>
15. Fahmi, M. Y., Muttaqin, A. D., Ardiansyah, R. E., Anggreini, R., Widyawati, S. S. L. (2025). Potential carbon content by mangrove forest along the coast-line of Trenggalek regency. *Ecological Engineering & Environmental Technology*, 26(1), 41–57. <https://doi.org/10.12912/27197050/195343>
 16. Feizizadeh, B. (2023). Machine learning data-driven approaches for land use/cover mapping and trend analysis using Google Earth Engine. *Journal of Environmental Planning and Management*, 66(3), 665–697. <https://doi.org/10.1080/09640568.2021.2001317>
 17. Gijisman, R., Horstman, E. M., Wal, D. van der,... (2021). Nature-based engineering: a review on reducing coastal flood risk with mangroves. In *Frontiers in Marine Science*. [frontiersin.org. https://doi.org/10.3389/fmars.2021.702412](https://doi.org/10.3389/fmars.2021.702412)
 18. Gilani, H. (2021). Evaluating mangrove conservation and sustainability through spatiotemporal (1990–2020) mangrove cover change analysis in Pakistan. *Estuarine Coastal and Shelf Science*, 249. <https://doi.org/10.1016/j.ecss.2020.107128>
 19. Goldberg, L., Lagomasino, D., Thomas, N.,... (2020). Global declines in human-driven mangrove loss. *Global Change Biology*. <https://doi.org/10.1111/gcb.15275>
 20. Hagger, V., Worthington, T. A., Lovelock, C. E.,... (2022). Drivers of global mangrove loss and gain in social-ecological systems. In *Nature communications*. [nature.com. https://www.nature.com/articles/s41467-022-33962-x](https://www.nature.com/articles/s41467-022-33962-x)
 21. Hoque, M. Z. (2020). Future impact of land use/land cover changes on ecosystem services in the lower meghna river estuary, Bangladesh. *Sustainability Switzerland*, 12(5). <https://doi.org/10.3390/su12052112>
 22. Hoque, M. Z. (2022). Monitoring Changes in land use land cover and ecosystem service values of dynamic saltwater and freshwater systems in coastal bangladesh by geospatial techniques. *Water Switzerland*, 14(15). <https://doi.org/10.3390/w14152293>
 23. Irwan, I., Rani, C., Jompa, J., Nurdin, N. (2024). Spatial and temporal dynamics of marine trophic status using the trophic index in Bone Bay, Indonesia. *Ecological Engineering & Environmental Technology*, 25(10), 181–193. <https://doi.org/10.12912/27197050/191786>
 24. Kaffle, S., Sandeep, K. C., Poudyal, B.,... (2023). Machine learning approach to detect land use land cover (LULC) change in Chure region of Sarlahi district, Nepal. In *Archives of Agriculture and Environmental Science*. [academia.edu. https://www.academia.edu/download/119531625/628-AAES-1413-1-10-20230625.pdf](https://www.academia.edu/download/119531625/628-AAES-1413-1-10-20230625.pdf)
 25. Kanniah, K. D. (2021). Remote sensing to study mangrove fragmentation and its impacts on leaf area index and gross primary productivity in the south of peninsular malaysia. *Remote Sensing*, 13(8). <https://doi.org/10.3390/rs13081427>
 26. Kauffman, J. B., Giovanonni, L., Kelly, J.,... (2020). Total ecosystem carbon stocks at the marine-terrestrial interface: Blue carbon of the Pacific Northwest Coast, United States. *Global Change Biology*. <https://doi.org/10.1111/gcb.15248>
 27. Krauss, K. W., Osland, M. J. (2020). Tropical cyclones and the organization of mangrove forests: a review. *Annals of Botany*. <https://academic.oup.com/aob/article-abstract/125/2/213/5585844>
 28. Li, W., Wang, L., Yang, X., Liang, T., Zhang, Q., Liao, X.,... (2022). Interactive influences of meteorological and socioeconomic factors on ecosystem service values in a river basin with different geomorphic features. *Science of The Total Environment*. <https://www.sciencedirect.com/science/article/pii/S0048969722016886>
 29. Liu, L., Wang, H., Yue, Q. (2020). China's coastal wetlands: Ecological challenges, restoration, and management suggestions. *Regional Studies in Marine Science*. <https://www.sciencedirect.com/science/article/pii/S2352485520304655>
 30. Maurya, K., Mahajan, S., Chaube, N. (2021). Remote sensing techniques: Mapping and monitoring of mangrove ecosystem—A review. In *Complex & Intelligent Systems*. Springer. <https://doi.org/10.1007/s40747-021-00457-z>
 31. Newton, A. (2020). Anthropogenic, Direct pressures on coastal wetlands. In *Frontiers in Ecology and Evolution*, 8. <https://doi.org/10.3389/fevo.2020.00144>
 32. Pande, C. B., Srivastava, A., Moharir, K. N.,... (2024). Characterizing land use/land cover change dynamics by an enhanced random forest machine learning model: a Google Earth Engine implementation. In *Environmental Sciences Europe*. Springer. <https://doi.org/10.1186/s12302-024-00901-0>
 33. Patil, A., Panhalkar, S. (2023). A comparative analysis of machine learning algorithms for land use and land cover classification using google earth engine platform. *Journal of Geomatics*. https://onlinejog.org/index.php/journal_of_geomatics/article/view/96
 34. Ravaoarinorotsihoarana, L. A., Ratefinjanahary, I., Aina, C.,... (2023). Combining traditional ecological knowledge and scientific observations to support mangrove restoration in Madagascar. In *Forests*. [mdpi.com. https://www.mdpi.com/1999-4907/14/7/1368](https://www.mdpi.com/1999-4907/14/7/1368)
 35. Sardar, P. (2021). Understanding the dynamics of landscape of greater Sundarban area using multi-layer perceptron Markov chain and landscape statistics approach. *Ecological Indicators*, 121. <https://doi.org/10.1016/j.ecolind.2020.106914>
 36. Sharma, S., MacKenzie, R. A., Tieng, T., Soben,

- K.,... (2020). The impacts of degradation, deforestation and restoration on mangrove ecosystem carbon stocks across Cambodia. *Science of the Total Environment* <https://www.sciencedirect.com/science/article/pii/S0048969719354099>
37. Sobhani, P., Danehkar, A. (2023). Evaluating and zoning of ecosystem services in mangrove forests of Khamir and Qeshm. *Town and Country Planning*. https://jtcp.ut.ac.ir/article_93351_en.html?lang=fa
38. Syahid, L. N., Sakti, A. D., Ward, R., Rosleine, D.,... (2023). Optimizing the spatial distribution of Southeast Asia mangrove restoration based on zonation, species and carbon projection schemes. *Estuarine, Coastal and Shelf Science*. <https://www.sciencedirect.com/science/article/pii/S0272771423002676>
39. Tinh, P. H., Hanh, N. T. H., Thanh, V. Van,... (2020). A comparison of soil carbon stocks of intact and restored mangrove forests in Northern Vietnam. *Forests*. <https://www.mdpi.com/739070>
40. Trialfhianty, T. I., Muharram, F. W., Quinn, C. H., Beger, M. (2022). Spatial multi-criteria analysis to capture socio-economic factors in mangrove conservation. *Marine Policy*. <https://www.sciencedirect.com/science/article/pii/S0308597X22001415>
41. Turschwell, M. P., Tulloch, V. J. D., Sievers, M.,... (2020). Multi-scale estimation of the effects of pressures and drivers on mangrove forest loss globally. *Biological Conservation*. <https://www.sciencedirect.com/science/article/pii/S0006320720306959>
42. Vimal, R., Navarro, L. M., Jones, Y., Wolf, F.,... (2021). The global distribution of protected areas management strategies and their complementarity for biodiversity conservation. *Biological Conservation*. <https://www.sciencedirect.com/science/article/pii/S0006320721000665>
43. Williams, L. (2022). Building an ecology of resilience through religious practice and community in northern Uganda. *Civil Wars*. <https://doi.org/10.1080/13698249.2022.2092685>
44. Zhang, B., Zhang, L., Chen, B., Deng, L., Fu, B., Yan, M.,... (2024). Assessment of mangrove health based on pressure–state–response framework in Guangxi Beibu Gulf, China. In *Ecological Indicators*. Elsevier. <https://www.sciencedirect.com/science/article/pii/S1470160X24011427>
45. Zhao, C. (2020). 10-m-resolution mangrove maps of China derived from multi-source and multi-temporal satellite observations. *ISPRS Journal of Photogrammetry and Remote Sensing*, 169, 389–405. <https://doi.org/10.1016/j.isprsjprs.2020.10.001>